

## Designed and Validation of In-House Head and Neck Phantom for Quality Assurance and Radiotherapy Dose Measurements

Mamta Mahur<sup>1,2\*</sup>, Munendra Singh<sup>2</sup>, Om Prakash Gurjar<sup>3</sup>, M K Semwal<sup>4</sup>

1. Department of Radiotherapy, Delhi State Cancer Institute, Dilshad Garden, Delhi – 110095, India.
2. Department of Physics, School of Basic Sciences & Research, Sharda University, Greater Noida, Uttar Pradesh- 201310, India.
3. Government Cancer Hospital, MGM Medical College, Indore-452001, India.
4. Army Hospital (Research & Referral), Delhi Cantonment, New Delhi-110010, India.

ARTICLE INFO	ABSTRACT
<b>Article type:</b> Original Paper	<b>Introduction:</b> In radiotherapy treatment of head and neck (H&N) cancers, more complex quality assurance checks and patient-specific dosimetry are required to ensure accuracy in modern technology. In this paper, a new cost-effective human tissue equivalent H&N phantom was designed to serve as an economical and adaptable tool for assessment and assurance of precise radiotherapy dose delivery.
<b>Article history:</b> Received: Feb 08, 2022 Accepted: Sep 18, 2022	<b>Material and Methods:</b> The phantom was designed using locally available paraffin wax and tissue-equivalent materials. Computed tomography (CT) images of the phantom were acquired using a conventional CT simulator and were registered with the images of a real patient having approximately similar physical dimensions. The geometric and attenuation properties of the structures in the phantom were studied and compared to the structures of the real patient.
<b>Keywords:</b> Paraffin Head and Neck Cancer Phantom Radiotherapy and Quality Assurance	<b>Results:</b> Hounsfield unit (HU) values of different structures of the phantom were compared to the values obtained from the CT images of a real patient and were found to be in good agreement. HU values obtained for the right, and left eye, brain, larynx, and bone shell were $7(\pm 10)$ HU, $6(\pm 9)$ , $30(\pm 14)$ HU, $-984(\pm 6)$ HU and $873(\pm 214)$ HU in phantom. Structures simulated in phantom agreed well on comparison regarding both their design and radiation properties with respect to real patient human tissues. Gamma analysis was performed for the axial dose plane at plan isocenter for both the calculated dose distribution in H&N phantom and the patient agrees for 98.79% passing rate for 3% /3mm criteria.
	<b>Conclusion:</b> The designed phantom depicts human anatomy and meets the requirements of tissue equivalence. The result shows that phantom has proved to be a cost-effective and valuable tool for accurate verification of dose distributions in regions of clinical and dosimetric interests.

► Please cite this article as:

Mahur M, Singh M, Gurjar P, Semwal M K. Designed and Validation of In-House Head and Neck Phantom for Quality Assurance and Radiotherapy Dose Measurements. Iran J Med Phys 2023; 20: 282-289. 10.22038/IJMP.2022.63407.2084.

### Introduction

Phantoms are one of the important tools to perform radiotherapy dosimetry and quality assurance (QA) procedure in a radiation department to ensure accuracy in dose delivery. For modern radiotherapy techniques, pretreatment dose verification is an important step. Different types of pretreatment patient-specific dosimetric QA techniques are available to ensure precise dose delivery. Usually, verification of this delivered dose is performed by replacing the patient with tissue equivalent material called phantom [1-3].

Water is the main component of the human body and is recommended as the reference medium for the measurement of absorbed doses in radiation therapy. Due to practical and technical issues related to the use of water, which is considered to be a standard phantom material according to the International Atomic Energy Agency (IAEA) [4-6], other solid materials like Polymethyl methacrylate (PMMA) or polystyrene materials are opted for to build the

homogeneous phantom and to mimic the dose distribution similar to the human body [3, 7]. But such materials are locally not available. These homogeneous phantoms are totally in standard geometric shape and do not reflect the different densities of structures as found in real patients [7-12]. Hence, the resulting dose distributions obtained from these homogeneous phantoms are totally different in their patterns as compared to the real patients. This dosimetry error contributes to the inaccurate and nonrealistic depiction of the clinical effects of delivered doses.

Some head and neck (H&N) phantoms e.g. Rando phantom and RPC (Radiological Physics Center) phantom which represent similar geometric structures as compared to real patients are commercially available but they are costly and unaffordable for most radiotherapy centers. In most of these phantom measurements, positions are fixed and involve the limitation of using various detectors to

\*Corresponding Author: Tel: +9971875902; Email: mamtamahur@gmail.com

verify doses at different positions [13]. These anthropomorphic phantoms allow the use of detectors like films and Metal oxide semiconductor field effect transistors (MOSFETs) for surface measurements. In Rando phantom, slots for insertion of thermoluminescent dosimeters (TLDs) in the form of a 3D array and provision for the insertion of film dosimeter are present to perform dosimetric verification in axial planes at specific distances [7,9,14-15]. These phantoms do not provide the provision for the insertion of other detectors like ionization chambers.

Different methods have been used in the past by researchers in developing anthropomorphic phantoms using various tissue-mimicking materials. Kim et al [16] constructed a 3D-printed spine QA phantom consisting of a high-density acrylic body phantom and a 3D-printed spine-shaped object. The doses computed on the patient-specific anthropomorphic phantom that was created were compared to the doses calculated on the original patient. Markis et al [17] designed a head phantom having external contour and bone structures of high-density bone-mimicking material. The resultant head phantom was filled with water, and computational and experimental evaluations were done to determine the degree of patient-to-phantom dosimetric equivalency. Zhang et al [18] fabricated a chest phantom via the 3D printing technique and filled the phantom with materials to simulate soft tissue and fat. Acrylonitrile butadiene styrene (ABS) was used in printing the fat and chest wall shell and the radiation equivalent material of ribs, sternum angle, and scapula were made with modified resin polymer material. To as closely mimic the actual patient and treatment geometry as possible, Oinam et al [19] created a homogeneous H&N phantom (Figure 1) using paraffin wax with no heterogeneities involved. Comparison was performed between the computed buildup doses from the Treatment planning system (TPS) and the corresponding measured doses in the phantom using thermoluminescent dosimeters (TLD 100). TLD-100 is a type of thermoluminescent dosimetry material made of Lithium Fluoride. Eng et al [20] performed the IMRT planned dose verification using a customized acrylic H&N phantom. The acrylic slabs were cut using electronic hand cutter and polished to make shape smooth. Gareth et al [21] developed a semi-anatomic Perspex phantom with provisions for the insertion of heterogeneities simulating air cavities in a range of fixed positions. The phantom was used for the verification of IMRT plans for the H&N. Akpochafor et al [22] designed in-house phantom, constructed in the shape of a block using Plexiglas and filled with water having the provision for hollow inserts for the ionization chamber and tissue equivalent materials.

Previously reported methods were either complicated as well as hard to be practically adopted

for clinical practice due to the involvement of advanced technologies used in manufacturing of anthropomorphic phantoms or the resulting phantoms were simple with no anatomical depiction of real patient. Also, it is difficult to reproduce and verify extreme clinical conditions such as presence of implants and prosthesis as found in some specific cases of patients. Presence of these metallic implants and prosthesis in treatment region complicates the dose calculation process in TPS, which can result into serious dosimetric errors. Hence, in order to stimulate individualized realistic clinical and measurement conditions, patient specific dosimetric phantoms are needed to ensure the accuracy of treatment.

The purpose of our study is to fabricate a cost-effective tissue equivalent H&N phantom that will achieve the goal of representing human anatomy along with the practicality of the use of different types of dosimeters. It can also be designed to adapt quickly to various clinical situations like the presence of metal artifacts caused by dental implants, prostheses, and non-uniformity of skin caused due to surgery, etc.

## Materials and Methods

For the construction of the phantom, material was chosen to meet the tissue equivalence requirements i.e. physical properties like density, electron density relative to water, linear attenuation coefficient relative to water and Computed Tomography (CT) density equivalent to human tissue as well as fast manufacturing process. It is evident from various studies that paraffin wax serves as an alternative of solid water phantom because of its similar dose absorption properties due to similar chemical composition, mass density and number of electrons to water [23-26]. The density and electron density (ED) of paraffin wax is  $0.9\text{g/cm}^3$  [27] and  $3.44 \times 10^{23}\text{e/g}$  respectively.

Different types of waxes were bought from area local market and were tested for comparing their HU (Hounsfield units) values and physical density. For this test CT images of waxes were acquired using a Biograph mCT Flow systems scanner (Siemens Healthcare, Germany). Hounsfield Unit (HU) values were further evaluated from various slices of the scanned images obtained at the CT scanner console.

For bone structure, bone shell with the help of 3D printer were constructed and filled with bone equivalent material. A conventional airy sponge was used to simulate the air-filled anatomical structures like trachea and paranasal sinus. Eyes were simulated by using conventional gel because the HU number of actual eye and the gel used was approximately same. The molten paraffin wax was then poured into and was allowed to solidify subsequently. The inhouse designed H&N phantom weight was approximately equivalent to human head with height of 19.7cm, length of 23.6cm and width of 14.5cm as the physical dimensions of the fabricated phantom.

After completion of the manufacturing process, phantom was assembled for further validation by

acquiring CT images data set with 1mm slice thickness at 120Kilovoltage (KV). The phantom was scanned along with immobilization aids like H&N base plate and head rest. The acquired CT images of H&N phantom were registered for image fusion using Monaco treatment planning system (TPS) version 5.11 (Elekta, Impac Medical System, Inc., USA) with one of the real patient CT images having similar physical features. Contours were drawn for normal structures like body contour, spine, eyes, brain, teeth larynx, mandible etc.

To evaluate the geometric accuracy of the inhouse designed H&N phantom, volume and mean ED of each contoured structures were compared. An arbitrary tumor volume was contoured on registered images of the H&N phantom and patient. For dosimetric evaluation, 3-Dimensional conformal radiotherapy (3DCRT) plan for treatment delivery was planned for both the real patient CT images and H&N phantom CT images data sets using Monaco TPS for 6 Megavoltage (MV) photon beam with the same beam arrangements and planning parameters. Dose calculation was performed for a prescribed dose of 40Gy in 20 fractions by using collapsed cone algorithm. Dosimetric characteristics were compared by evaluating doses to different structures from a Dose-volume histogram (DVH). Also, two-dimensional dose difference maps were compared and evaluated using the gamma analysis method for the transverse dose plane at the planning isocenter.

**Results**

Table 1 summarizes the comparison of HU values evaluated from CT images of different waxes from different slices. The mean HU value was approximately -50HU for Wax4 (paraffin wax) which was appropriate for reproduction of soft tissue. Rahman et al [25] have studied and compared the dosimetric property of paraffin wax with those of solid phantom and PMMA phantom and found paraffin wax to be as good alternative of solid water phantom because of their proximity to the dose absorption property of water. They found the deviation to be within ±3% for 6MV in dose absorption comparison to that of water.

Table 1. Overview of HU values of different waxes

Material	ED value(e/cm <sup>3</sup> )	Range of HU values
Wax1(bee wax)	0.98 to 1.02	-20 to 60
Wax2 (yellow wax)	1.017 to 0.952	-30 to -112
Wax3(Refined wax)	0.994 to 1.043	-60 to 3
Wax4(paraffin wax)	1.005 to 0.992	-46 to -62
Wax5(Candle wax)	1.024 to 0.959	-21 to -100



Figure 1. Inhouse designed H&N phantom

After completion of the manufacturing process of H&N phantom (Figure 1) acquired CT images of the phantom were transferred to Monaco TPS for further validation. Figure 2 shows the example of CT images of constructed H&N phantom. HU values and ED values of structures contoured were evaluated using the image analysis tool in Monaco TPS. Mean HU and mean ED values along with standard deviation for various contoured structures like larynx, eye, spine, teeth, and bone were obtained and are presented in Table 2. The obtained HU values of the phantom were compared to the values obtained from the CT images of the real patient and were found to be in good agreement with respective real human tissues. Comparison of the volume of contoured structures such as eye, brain, external body, and larynx are presented in Table 3. Eyes simulated in phantom have larger volume in comparison to that of patient.

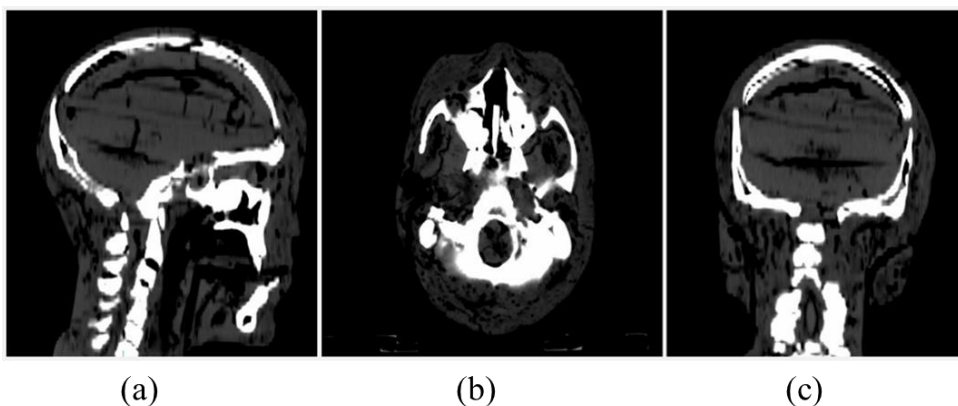


Figure 2. (a) Sagittal, (b) transverse and (c) coronal sections of the CT images of the constructed H&N phantom

Table 2. Comparison of Mean HU and mean ED values of various structures

Structures	Patient		Phantom	
	Mean HU( $\pm$ SD)	mean ED( $\pm$ SD)	Mean HU( $\pm$ SD)	mean ED( $\pm$ SD)
Right eye	7( $\pm$ 10)	1.047( $\pm$ 0.008)	5( $\pm$ 7)	1.045( $\pm$ 0.005)
Left eye	6( $\pm$ 9)	1.046( $\pm$ 0.007)	4( $\pm$ 9)	1.046( $\pm$ 0.007)
Brain	30( $\pm$ 14)	1.061( $\pm$ 0.008)	-43( $\pm$ 8)	1.007( $\pm$ 0.006)
Teeth	1339( $\pm$ 150)	1.815( $\pm$ 0.094)	850( $\pm$ 22)	1.508( $\pm$ 0.013)
Larynx	-984( $\pm$ 6)	0.017( $\pm$ 0.006)	-858( $\pm$ 7)	0.195( $\pm$ 0.007)
Bone shell	873( $\pm$ 214)	1.527( $\pm$ 0.013)	1161( $\pm$ 125)	1.7031( $\pm$ 0.077)
Spine	26( $\pm$ 40)	1.056( $\pm$ 0.02)	-23( $\pm$ 18)	1.007( $\pm$ 0.014)

Table 3. Volumes in cc of various contoured structures.

Structure	Volume in cc	
	Patient	Phantom
External body	4665.392	4950.059
Rt eye	9.114	15.44
Lt eye	7.534	13.89
Brain	1374.6	1157.77
Spine	11.747	10.23
Mandible	56.456	71.976
Larynx	30.374	37.969

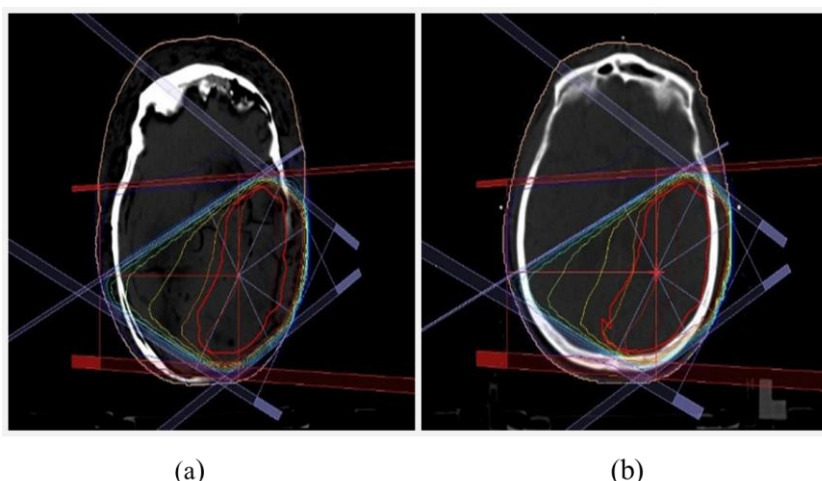


Figure 3. Dose distribution at plan isocenter in transverse plane for (a) H&N phantom and (b) patient

Table 4. Comparison of doses evaluated for different structures

Structure		Patient (Dose in cGy)	Phantom (Dose in cGy)
External body	Max dose	4498	4526.6
Right eye	Max dose	899.6	957.7
Left eye	Max dose	49.3	95.4
Brain	Mean dose	1551.7	1779.1
Tumor	D95 (dose to 95% Volume)	3672	3668
	D99 (dose to 99% Volume)	3474.7	3474.87

Dosimetric comparison of 3DCRT plans calculated for both H&N phantom and patient showed similar dose distribution. Figure 3 shows the dose distribution at isocenter in transverse plane for H&N phantom and patient respectively. 236 Monitor units (MU) and 246 MU were obtained per fraction for the calculated plans for phantom and patient respectively. Table 4 shows the doses evaluated

for the different structures from DVH and it is evident that doses obtained from H&N phantom are slightly higher.

Gamma analysis is typically used to judge the agreement between two dose distributions usually obtained from the treatment plan and QA dose measurements [28]. Here in this paper, we have used gamma analysis method using OmniPro IMRT software version 1.7.00114 (IBA Dosimetry, Germany) to compare the two calculated dose

planes obtained from 3DCRT radiotherapy plans calculated on phantom and patient CT images. Figure 4 shows the Gamma analysis performed for transverse dose plane at planning isocenter for both the calculated dose distribution in H&N phantom and patient agrees for 98.79% passing rate for 3% /3mm criteria.

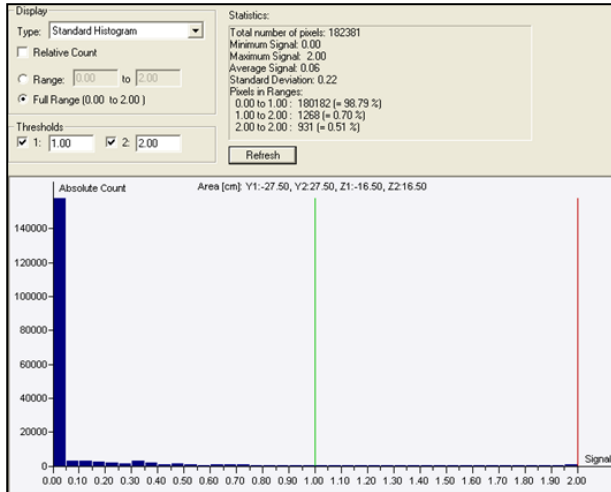


Figure 4. Result of gamma evaluation of dose distribution of 3DCRT plan in H&N phantom and patient

## Discussion

Surgical resection of primary tumor followed by chemotherapy and radiotherapy are the main treatment regime for H&N cancer patients with locally advanced tumors. Significant toxicities and functional restrictions are the common outcome of this multimodality treatment [29-33]. These toxicities significantly affect the patient's quality life and lead to other related complications. To reduce radiation induced toxicities modern techniques like Intensity-modulated radiation therapy (IMRT) and Volumetric modulated arc therapy (VMAT) are used [34-35]. But the verification of planned doses for accuracy becomes a challenging task for individual clinical conditions like presence of dental and metal artifacts. The verification of delivered radiotherapy dose can be performed more appropriately in a phantom.

Therefore, a new cost-effective 3D phantom was especially designed for the verification of planned treatment doses in radiotherapy of H&N cancers. The phantom can be used to perform dosimetry using films, ion chamber, TLDs, optically stimulated luminescent dosimeters (OSLDs) and mosfet dosimeters. The inhouse designed phantom met the predefined requirements of human tissue equivalence. The CT number values for contoured structures and their respective volumes were closer to the values of a real patient.

On comparison of dose fluence from the transverse plane at the isocenter slice, the two plans based on the real patient and H&N phantom, showed similar dose distribution. Figure 5 shows the comparison of isodose

distributions in H&N phantom and patient in transverse slice at isocenter plane as obtained from OmniPro IMRT software. High dose region and low dose region for calculated dose distribution in phantom and patient are similar as evident from the overlapping isodose lines. Large dose difference was observed in high dose region near border of external body contour and target. Most of the center region of tumor showed good agreement with a dose difference within 3% as evaluated from Gamma analysis. Dose statistics and DVH of calculated plans were quite similar for the contoured structures except in the case of eyes as there is disparity in volumes of eyes simulated. Nevertheless, the dosimetric characteristics of the phantom were well matched with those of the patient with a dose difference within  $\pm 5\%$ . The result obtained shows that the deviation between the monitor units of the plan calculated on H&N phantom and the patient were found to be 4.06%. Also, Dose indices values of 95% and 99% volume in case of tumor were well matched.

Rahman et al [26], have reported deviations in measured absorbed dose values from (-2.7)% to 1% and (-0.1)% to 2.4 % for the 6MV and 15MV photon beam respectively, for solid paraffin wax cube phantom when compared to water phantom and verified that paraffin wax phantom represents an acceptable and practical alternative to solid water phantom. Amour et al [36] studied the Percentage depth dose (PDD) values for water and beeswax phantoms and found to be in agreement with that of British journal of radiology (BJR) data. It was found that the use of depth dose and isodose curve of beeswax phantom in dose planning can be a good tissue equivalent substitute. A study by Kamomae et al [37] compared the phantom shape, CT value, and absorbed doses between the actual and in house designed 3D-printed phantoms by using Radiophotoluminescence (RPL) glass dosimeters and stated that fabrication quality can be improved by optimizing the printing parameters and employing high-performance devices and software. Their results demonstrated the feasibility of the 3D-printed phantom for artificial in vivo dosimetry in radiotherapy quality assurance. Dongruyl et al [38] developed a patient-specific dosimetric phantom using three-dimensional printing (PSDP\_3DP) and analyzed its geometrical and dosimetric accuracy. Three different types of material densities like UV- curable acrylic plastic (UVAP), plastic powder, and titanium were used to create the external body, spine and the internal body was filled with agar liquid only. The registered CT of the PSDP\_3DP was found to be well matched with that of the real patient CT in the axial, coronal, and sagittal planes. The dosimetric characteristics of the PSDP\_3DP were compared with the patient plan by applying the same beam parameters as for the patient and were found to be comparable to those of a real patient.

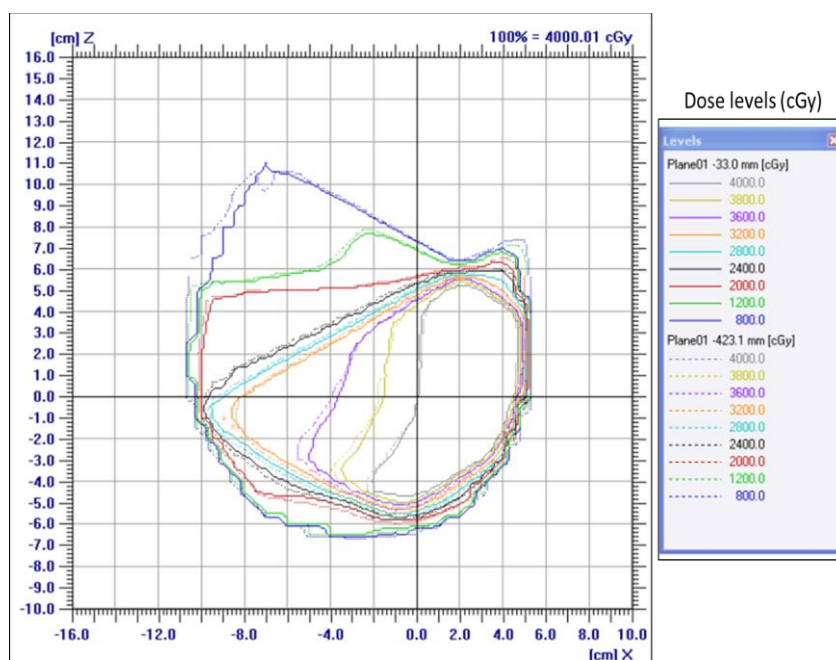


Figure 5. Comparison of isodose distributions in H&N phantom and patient 3DCRT plan (Solid lines: Patient; dotted lines: H&N Phantom)

A study by Na et al [39] investigated radiotherapeutic valuation of Paraffin Wax as an ideal material for oral cavity as a compensator in radiotherapy for patients with oral cancer. Radiation dose attenuation ratios were reported to be 0.21 to 0.39% for Paraffin Wax.

However, no study has been conducted so far to evaluate the dosimetry aspect of paraffin wax H&N phantom with heterogeneous structures representing human anatomy using Monaco TPS.

As accurate dosimetric quality assurance procedure requires a patient specific dosimetry phantom that generates the same dose distribution as of in real patient. High end casting and computerized milling machines are typically used to manufacture such standard dosimetry phantoms. We have designed this cost-effective phantom with limited resources. Replicating geometric features of human tissues such as internal structures of an organ is challenging using the molding technique. During fabrication of H&N phantom minor problems were faced regarding filling of the phantom due to the presence of small spaces caused by air bubbles after setting of the wax. It is recommended to keep the phantom in uniform temperature conditions as the structure of the phantom may suffer from deformity in case of high-temperature fluctuations. For future work, it can be proposed to explore the dosimetry aspects with high energy photon beams and verification of new modern technology delivery techniques using the designed H&N phantom.

## Conclusion

In this study, a physical H&N phantom was designed which has human equivalent anatomical shape, size, weight and other physical aspects. HU values from the CT images of the phantom were similar to that of human body. This new cost-effective tissue equivalent

fabricated phantom can serve as a useful tool in validation and assessment of precise delivery of radiation dose in H&N cancer patients for specific clinical situations.

## Acknowledgment

The work has been supported by Delhi state cancer institute.

## References

1. Ma CM, Jiang SB, Pawlicki T, Chen Y, Li JS, Deng J, et al. A quality assurance phantom for IMRT dose verification. Proceedings of the 22nd Annual International Conference of the IEEE Engineering in Medicine and Biology Society (Cat. No. 00CH37143). 2000; 2:1180-3.
2. Musolino SV. Absorbed dose determination in external beam radiotherapy: an international code of practice for dosimetry based on standards of absorbed dose to water; technical reports series (No. 398). 2000.
3. Podgorsak EB. Radiation oncology physics: A Handbook for Teachers and Students. 2005.
4. IAEA, Technical Reports Series No. 277. Absorbed Dose Determination in Photon and Electron Beams. IAEA, Vienna (2nd Edition in 1997). 1987.
5. Khan FM, Gibbons JP. Khan's the physics of radiation therapy. Lippincott Williams & Wilkins; 2014.
6. Andreo P, Cunningham JR, Hohlfield K, Svensson H. Absorbed dose determination in photon and electron beams. An international Code of Practice. 1987.
7. DeWerd LA. The phantoms of medical and health physics. Kissick M, editor. Berlin: Springer; 2014.
8. Tino R, Yeo A, Leary M, Brandt M, Kron T. A systematic review on 3D-printed imaging and dosimetry phantoms in radiation therapy.

- Technology in cancer research & treatment. 2019 Sep 12;18:1533033819870208.
9. McGarry CK, Grattan LJ, Ivory AM, Leek F, Liney GP, Liu Y, et al. Tissue mimicking materials for imaging and therapy phantoms: a review. *Physics in Medicine & Biology*. 2020 Dec 16;65(23):23TR01.
  10. Ezzell GA, Burmeister JW, Dogan N, LoSasso TJ, Mechalakos JG, Mihailidis D, et al. IMRT commissioning: multiple institution planning and dosimetry comparisons, a report from AAPM Task Group 119. *Medical physics*. 2009 Nov;36(11):5359-73.
  11. Ju SG, Han Y, Kum O, Cheong KH, Shin EH, Shin JS, et al. Comparison of film dosimetry techniques used for quality assurance of intensity modulated radiation therapy. *Medical physics*. 2010 Jun;37(6Part1):2925-33.
  12. Ravichandran R, Bhasi S, Binukumar JP, Davis CA. Need of patient-specific quality assurance and pre-treatment verification program for special plans in radiotherapy. *Journal of Medical Physics/Association of Medical Physicists of India*. 2011 Jul;36(3):181.
  13. Molineu A, Followill DS, Balter PA, Hanson WF, Gillin MT, Huq MS, et al. Design and implementation of an anthropomorphic quality assurance phantom for intensity-modulated radiation therapy for the Radiation Therapy Oncology Group. *International Journal of Radiation Oncology\* Biology\* Physics*. 2005 Oct 1;63(2):577-83.
  14. Maulana A, Pawiro SA. Dosimetry verification on VMAT and IMRT radiotherapy techniques: In the case of prostate cancer. In *Journal of Physics: Conference Series 2016 Mar 1 (Vol. 694, No. 1, p. 012010)*. IOP Publishing.
  15. Tazehmahalleh FE, Gholamhosseinian H, Layegh M, Tazehmahalleh NE, Esmaily H. Determining rectal dose through cervical cancer radiotherapy by 9 MV photon beam using TLD and XR type T GAFCHROMIC® Film. *Iran. J. Radiat. Res*. 2008 Dec 1;6(3):129-34.
  16. Kim MJ, Lee SR, Lee MY, Sohn JW, Yun HG, Choi JY, et al. Characterization of 3D printing techniques: Toward patient specific quality assurance spine-shaped phantom for stereotactic body radiation therapy. *PloS one*. 2017 May 4;12(5):e0176227.
  17. Makris DN, Pappas EP, Zoros E, Papanikolaou N, Saenz DL, Kalaitzakis G, et al. Characterization of a novel 3D printed patient specific phantom for quality assurance in cranial stereotactic radiosurgery applications. *Physics in Medicine & Biology*. 2019 May 10;64(10):105009.
  18. Zhang F, Zhang H, Zhao H, He Z, Shi L, He Y, et al. Design and fabrication of a personalized anthropomorphic phantom using 3D printing and tissue equivalent materials. *Quantitative imaging in medicine and surgery*. 2019 Jan;9(1):94.
  19. Oinam AS, Singh L. Verification of IMRT dose calculations using AAA and PBC algorithms in dose buildup regions. *Journal of applied clinical medical physics*. 2010 Sep;11(4):105-21.
  20. Eng KY, Kandaiya S, Yahaya NZ. Radiotherapy dose verification on a customised head and neck perspex phantom. In *Journal of Physics: Conference Series*. 2017; 851(1): 012020.
  21. Webster GJ, Hardy MJ, Rowbottom CG, Mackay RI. Design and implementation of a head-and-neck phantom for system audit and verification of intensity-modulated radiation therapy. *Journal of Applied Clinical Medical Physics*. 2008 Mar;9(2):46-56.
  22. Akpochafor MO, Aweda MA, Ibitoye AZ, Adeneye SO, Iloputaife C, Omojola AD. Verification of a treatment planning system using an in-house designed head and neck phantom. *Archives of Physics Research*. 2013;4(6):1-8.
  23. Verma TR, Painuly NK, Tyagi M, Johny D, Gupta R, Bhatt ML. Validation of the gel & wax boluses and comparison of their dosimetric performance with virtual bolus. *Journal of Biomedical Physics & Engineering*. 2019 Dec;9(6):629.
  24. Amour K, Maleka P, Maunda K, Mazunga M, Msaki P. Verification of Depth Dose Curves Derived on Beeswax, Paraffin and Water Phantoms Using FLUKA Monte Carlo Code. *Tanzania Journal of Science*. 2020 Oct 31;46(3):923-30.
  25. Rahman MA, Jamil HM, Elius IB, Khan AHAN, Haydar MA. Design and fabrication of wax cube phantoms for the assessment of paraffin wax as phantom material for radiotherapy. *Nuclear science and applications*. 2020; 29(1&2):37-41.
  26. Rahman MA, Bhuiyan MT, Rahman MM, Chowdhury MN. Comparative study of absorbed doses in different phantom materials and fabrication of a suitable phantom. *Malaysian Journal of Medical and Biological Research*. 2018 Jun 30;5(1):19-24.
  27. Hadi H and Ali Abed F. Introducing a simple tissue equivalent anthropomorphic phantom for radiation dosimetry in diagnostic radiology and radiotherapy. *Journal of paramedical sciences*. 2011; 2 (4) : 25-9. DOI:10.22037/JPS.V2I4.2718.
  28. Low DA, Moran JM, Dempsey JF, Dong L, Oldham M. Dosimetry tools and techniques for IMRT. *Medical physics*. 2011 Mar;38(3):1313-38.
  29. Rades D, Kronemann S, Meyners T, Bohlen G, Tribius S, Kazic N, et al. Comparison of four cisplatin-based radiochemotherapy regimens for nonmetastatic stage III/IV squamous cell carcinoma of the head and neck. *Int. J. Radiat. Oncol. Biol. Phys*. 2011 Jul 15;80(4):1037-44.
  30. Tribius S, Kronemann S, Kilic Y, Schroeder U, Hakim S, Schild SE, et al. Radiochemotherapy including cisplatin alone versus cisplatin+ 5-fluorouracil for locally advanced unresectable stage IV squamous cell carcinoma of the head and neck. *Strahlentherapie und Onkologie*. 2009 Oct 1;185(10):675.
  31. Bernier J, Dommenege C, Ozsahin M, Matuszewska K, Lefebvre JL, Greiner RH, et al. Postoperative irradiation with or without concomitant chemotherapy for locally advanced head and neck cancer. *New England Journal of Medicine*. 2004 May 6;350(19):1945-52.
  32. Cooper JS, Pajak TF, Forastiere AA, Jacobs J, Campbell BH, Saxman SB, et al. Postoperative concurrent radiotherapy and chemotherapy for high-risk squamous-cell carcinoma of the head and neck. *New England Journal of Medicine*. 2004 May 6;350(19):1937-44.
  33. Rades D, Fehlauer F, Wroblewski J, Albers D, Schild SE, Schmidt R. Prognostic factors in head-and-neck cancer patients treated with surgery followed by intensity-modulated radiotherapy (IMRT), 3D-conformal radiotherapy, or conventional

- radiotherapy. *Oral oncology*. 2007 Jul 1;43(6):535-43.
34. Franzese C, Fogliata A, Franceschini D, Clerici E, D'AGOSTINO GI, Navarria P, et al. Treatment: outcome and toxicity of volumetric modulated arc therapy in oropharyngeal carcinoma. *Anticancer Research*. 2016 Jul 1;36(7):3451-7.
  35. Bucci MK, Bevan A, Roach III M. Advances in radiation therapy: conventional to 3D, to IMRT, to 4D, and beyond. *CA: a cancer journal for clinicians*. 2005 Mar;55(2):117-34.
  36. Amour K, Maleka P, Maunda K, Mazunga M, Msaki P. Verification of Depth Dose Curves Derived on Beeswax, Paraffin and Water Phantoms Using FLUKA Monte Carlo Code. *Tanzania Journal of Science*. 2020 Oct 31;46(3):923-30.
  37. Kamomae T, Shimizu H, Nakaya T, Okudaira K, Aoyama T, Oguchi H, et al. Three-dimensional printer-generated patient-specific phantom for artificial in vivo dosimetry in radiotherapy quality assurance. *Physica medica*. 2017 Dec 1;44:205-11.
  38. Oh D, Hong CS, Ju SG, Kim M, Koo BY, Choi S, et al. Development of patient-specific phantoms for verification of stereotactic body radiation therapy planning in patients with metallic screw fixation. *Scientific reports*. 2017 Jan 19;7(1):40922.
  39. Na KS, Seo SJ, Lee JH, Yoo SH. Radiotherapeutic Valuation of Paraffin Wax for Patients with Oral Cancer. *The Journal of Korean Society for Radiation Therapy*. 2011;23(1):41-9.